Science
AAAS

Membrane Proteins of the Endoplasmic Reticulum Induce High-Curvature Tubules

Junjie Hu, *et al.*

Science **319**, 1247 (2008);
DOI: 10.1126/science.1153634

Science (print ISSN 0036-8075; online ISSN 1095-9203) is published weekly, except the last week in December, by the American Association for the Advancement of Science, 1200 New York Avenue NW, Washington, DC 20005.

spontaneous negative curvature by creating an area difference between the membrane leaflets. Another cone-shaped lipid, lysobisphosphatidic acid, induces the formation of internal vesicles in liposomes (*23*). This lipid, which is absent from exosomes (*16*), may regulate biogenesis and dynamics of ILVs along the degradative pathway (*24*). Ceramide, in contrast, seems to be used for the generation of another population of ILVs that are not destined for transport to the lysosomes but are secreted as one class of exosomes.

References and Notes

1. R. C. Piper, D. J. Katzmann, *Annu. Rev. Cell Dev. Biol.* **23**, 519 (2007).
2. J. Gruenberg, H. Stenmark, *Nat. Rev. Mol. Cell Biol.* **5**, 317 (2004).
3. C. Thery, L. Zitvogel, S. Amigorena, *Nat. Rev. Immunol.* **2**, 569 (2002).
4. W. Stoorvogel, M. J. Kleijmeer, H. J. Geuze, G. Raposo, *Traffic* **3**, 321 (2002).
5. G. van Niel, I. Porto-Carreiro, S. Simoes, G. Raposo, *J. Biochem.* **140**, 13 (2006).
6. K. Trajkovic *et al.*, *J. Cell Biol.* **172**, 937 (2006).
7. A. de Gassart, C. Geminard, B. Fevrier, G. Raposo, M. Vidal, *Blood* **102**, 4336 (2003).
8. B. Fevrier *et al.*, *Proc. Natl. Acad. Sci. U.S.A.* **101**, 9683 (2004).
9. H. Stenmark *et al.*, *EMBO J.* **13**, 1287 (1994).
10. C. Raiborg *et al.*, *Nat. Cell Biol.* **4**, 394 (2002).
11. C. Raiborg, J. Wesche, L. Malerod, H. Stenmark, *J. Cell Sci.* **119**, 2414 (2006).
12. J. H. Hurley, S. D. Emr, *Annu. Rev. Biophys. Biomol. Struct.* **35**, 277 (2006).
13. R. L. Williams, S. Urbe, *Nat. Rev. Mol. Cell Biol.* **8**, 355 (2007).
14. J. E. Garrus *et al.*, *Cell* **107**, 55 (2001).
15. R. Goila-Gaur, D. G. Demirov, J. M. Orenstein, A. Ono, E. O. Freed, *J. Virol.* **77**, 6507 (2003).
16. R. Wubbolts *et al.*, *J. Biol. Chem.* **278**, 10963 (2003).
17. B. Brügger *et al.*, *Proc. Natl. Acad. Sci. U.S.A.* **103**, 2641 (2006).
18. C. J. Clarke *et al.*, *Biochemistry* **45**, 11247 (2006).
19. J. M. Holopainen, M. I. Angelova, P. K. Kinnunen, *Biophys. J.* **78**, 830 (2000).
20. X. Zha *et al.*, *J. Cell Biol.* **140**, 39 (1998).
21. R. Li, E. J. Blanchette-Mackie, S. Ladisch, *J. Biol. Chem.* **274**, 21121 (1999).
22. E. Gulbins, R. Kolesnick, *Oncogene* **22**, 7070 (2003).
23. H. Matsuo *et al.*, *Science* **303**, 531 (2004).
24. F. G. van der Goot, J. Gruenberg, *Trends Cell Biol.* **16**, 514 (2006).

25. We are grateful to R. Bittman, D. Caplan, M. Zerial, D. Arndt-Jovin, U. Coskun, P. Keller, D. Cutler, P. Burfeind, and H. Stenmark for providing reagents and R. White for help with RNAi experiments. The work was supported by the Deutsche Forschungsgemeinschaft (SFB 523, GRK521).

Supporting Online Material

www.sciencemag.org/cgi/content/full/319/5867/1244/DC1
Materials and Methods
SOM Text
Figs. S1 to S12
References

19 November 2007; accepted 8 January 2008
10.1126/science.1153124

Membrane Proteins of the Endoplasmic Reticulum Induce High-Curvature Tubules

Junjie Hu,[1] Yoko Shibata,[1] Christiane Voss,[2] Tom Shemesh,[3] Zongli Li,[4] Margaret Coughlin,[5] Michael M. Kozlov,[3] Tom A. Rapoport,[1]* William A. Prinz[2]*

The tubular structure of the endoplasmic reticulum (ER) appears to be generated by integral membrane proteins, the reticulons and a protein family consisting of DP1 in mammals and Yop1p in yeast. Here, individual members of these families were found to be sufficient to generate membrane tubules. When we purified yeast Yop1p and incorporated it into proteoliposomes, narrow tubules (~15 to 17 nanometers in diameter) were generated. Tubule formation occurred with different lipids; required essentially only the central portion of the protein, including its two long hydrophobic segments; and was prevented by mutations that affected tubule formation in vivo. Tubules were also formed by reconstituted purified yeast Rtn1p. Tubules made in vitro were narrower than normal ER tubules, due to a higher concentration of tubule-inducing proteins. The shape and oligomerization of the "morphogenic" proteins could explain the formation of the tubular ER.

How the characteristic shape of an organelle is generated and maintained is largely unknown. The endoplasmic reticulum (ER), for example, consists of continuous membrane sheets and tubules (*1*, *2*), but it is unclear how these domains are made and kept morphologically distinct. The tubules are interconnected in a polygonal network and have diameters ranging from ~30 nm in *Saccharomyces cerevisiae* (*3*) to ~50 nm in mammals (*4*). The most plausible models for shaping ER tubules are based on mechanisms that generate or stabilize the high membrane curvature seen in cross sections. A curvature-stabilizing role has been suggested for a class of integral membrane proteins, the reticulons and a protein family that includes DP1 in mammals and Yop1p in yeast (*5*). These proteins are found in most, if not all, eukaryotic cells. They form homo- and heterooligomers and localize exclusively to ER tubules. Their overexpression generates long, unbranched tubules, and their deletion in yeast leads to the loss of tubular ER. The reticulon and Yop1p (DP1) families are not related in sequence, but they each contain a conserved domain of ~200 amino acids that includes two hydrophobic segments, which seem to form a hairpin in the membrane. It remains unclear whether the reticulons or Yop1p (DP1) are sufficient for tubule formation and how they might deform the membrane.

[1]Howard Hughes Medical Institute and Department of Cell Biology, Harvard Medical School, 240 Longwood Avenue, Boston, MA 02115, USA. [2]Laboratory of Cell Biochemistry and Biology, National Institute of Diabetes and Digestive and Kidney Disorders (NIDDK), National Institutes of Health, Bethesda, MD 20892, USA. [3]Department of Physiology and Pharmacology, Sackler Faculty of Medicine, Tel Aviv University, Ramat Aviv, 69978 Tel Aviv, Israel. [4]Department of Cell Biology, Harvard Medical School, 240 Longwood Avenue, Boston, MA 02115, USA. [5]Department of Systems Biology, Harvard Medical School, 240 Longwood Avenue, Boston, MA 02115, USA.

*To whom correspondence should be addressed. E-mail: tom_rapoport@hms.harvard.edu (T.A.R.); wprinz@helix.nih.gov (W.A.P.)

We first tested whether the reticulon and Yop1p (DP1) proteins would each generate membrane tubules when reconstituted with lipids into proteoliposomes. Yop1p was purified from *S. cerevisiae* with a cleavable N-terminal histidine (His) tag in the detergent lauryldimethylamine-*N*-oxide (LDAO) (Fig. 1A) (*6*). After cleavage of the His tag, *Escherichia coli* polar lipids were added, and the detergent was removed with Biobeads to generate proteoliposomes. At early time points during the reconstitution reaction, small vesicles and short tubules were seen by negative-stain electron microscopy (EM), both with a diameter of ~17 nm (Fig. 1B). Over the course of a day, the vesicles disappeared and the tubules grew in length, reaching several hundred nanometers, but their diameter remained the same (Fig. 1C). The tubules occasionally had branch points (Fig. 1C), which indicated that the lipid bilayers could branch or fuse during reconstitution. No tubules were seen when the lipids were omitted (Fig. 1D). In the absence of protein, round liposomes with heterogeneous size were generated (Fig. 1E). Yop1p formed tubules of identical diameter when reconstituted with other lipids (fig. S1), which suggested that the protein was primarily responsible for the shape of the proteoliposomes.

Next, we tested whether yeast reticulon Rtn1p could also induce tubules in vitro. Tubules were indeed seen in negative-stain EM when purified Rtn1p (Fig. 1F) was mixed with *E. coli* polar lipids and the detergent was removed by dialysis (Fig. 1G). The diameter of these tubules was about the same as with Yop1p, but bulges were frequently observed. When the detergent was removed by Biobeads, Rtn1p tubules were not generated, whereas, with Yop1p, both Biobeads and dialysis resulted in tubule formation. Because Rtn1p was less efficient than Yop1p in forming tubules, most of the subsequent experiments were performed with Yop1p.

Increasing the lipid concentration or decreasing the protein concentration in the reconstitution reaction resulted in fewer Yop1p tubules and an increased number of large vesicles (table

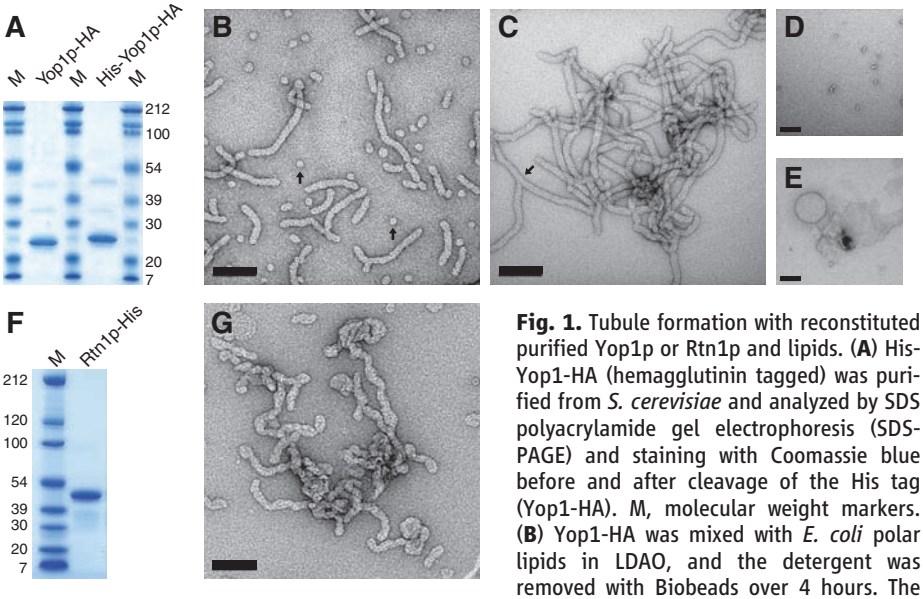

Fig. 1. Tubule formation with reconstituted purified Yop1p or Rtn1p and lipids. (**A**) His-Yop1-HA (hemagglutinin tagged) was purified from *S. cerevisiae* and analyzed by SDS polyacrylamide gel electrophoresis (SDS-PAGE) and staining with Coomassie blue before and after cleavage of the His tag (Yop1-HA). M, molecular weight markers. (**B**) Yop1-HA was mixed with *E. coli* polar lipids in LDAO, and the detergent was removed with Biobeads over 4 hours. The proteoliposomes were analyzed by negative-stain EM. Arrows indicate small vesicles. (**C**) As in (B), but after one day. The arrow indicates a branch point. (**D**) As in (B), but with protein only. (**E**) As in (B), but with lipid only. (**F**) Rtn1-His was purified from *S. cerevisiae* and analyzed by SDS-PAGE and Coomassie staining. (**G**) Rtn1-His was reconstituted with *E. coli* polar lipids in Fos-choline-12. The detergent was removed by dialysis for 1 week. Scale bars, 100 nm.

S1). The segregation of excess lipid from the tubules suggests that Yop1p self-associates during detergent removal and cannot easily be diluted in the plane of the membrane. Both Rtn1p and Yop1p indeed have the propensity to form oligomers. Up to five molecules could be cross-linked using a bifunctional cross-linker (fig. S2, A and B). Ladders of Yop1p oligomers were formed both with tubules generated in vitro and with native membranes (fig. S2A). Also, Yop1p solubilized from yeast membranes by digitonin migrated in sucrose gradients as oligomers containing about eight molecules (fig. S2C). The oligomers dissociated in LDAO but were resistant to high salt, which suggested that they are formed mainly through hydrophobic interactions.

Reconstituted Yop1p tubules sedimented rapidly in sucrose-gradient centrifugation experiments; the peak fractions contained almost all the Yop1p protein added to the reconstitution (fig. S3). In contrast, as expected, pure lipids or Yop1p in detergent stayed close to the top of the gradient. The gradient-purified tubules contain a lipid-to-protein molar ratio of ~10:1 (*6*). Although the protein molecules must be densely packed in the tubules, they did not show a regular arrangement in negative-stain EM.

Fig. 2. Correlation between tubule formation in vitro and in vivo. (**A**) Yop1-HA, His-Yop1-HA, or Yop1_ΔC1 were reconstituted as in Fig. 1B. Scale bars, 100 nm. (**B**) His-tagged Rtn1p wild type or M91 mutant [mutations: H7Y, K48I, T127I, I137P, and N277Y (*26*)] were reconstituted as in Fig. 1G. Scale bars, 100 nm. (**C**) The ER was visualized in yeast cells lacking Rtn1p, Rtn2p, and Yop1p by expressing a green fluorescent protein (GFP) fusion to Sec63p. The cells also contained either an empty vector, or centromere (CEN) plasmids expressing Yop1-HA, His-Yop1-HA, Yop1_ΔC1, Rtn1-His, or M91-His under the endogenous promoters. The microscope was focused at either the center or periphery of the cells. Scale bars, 1 μm.

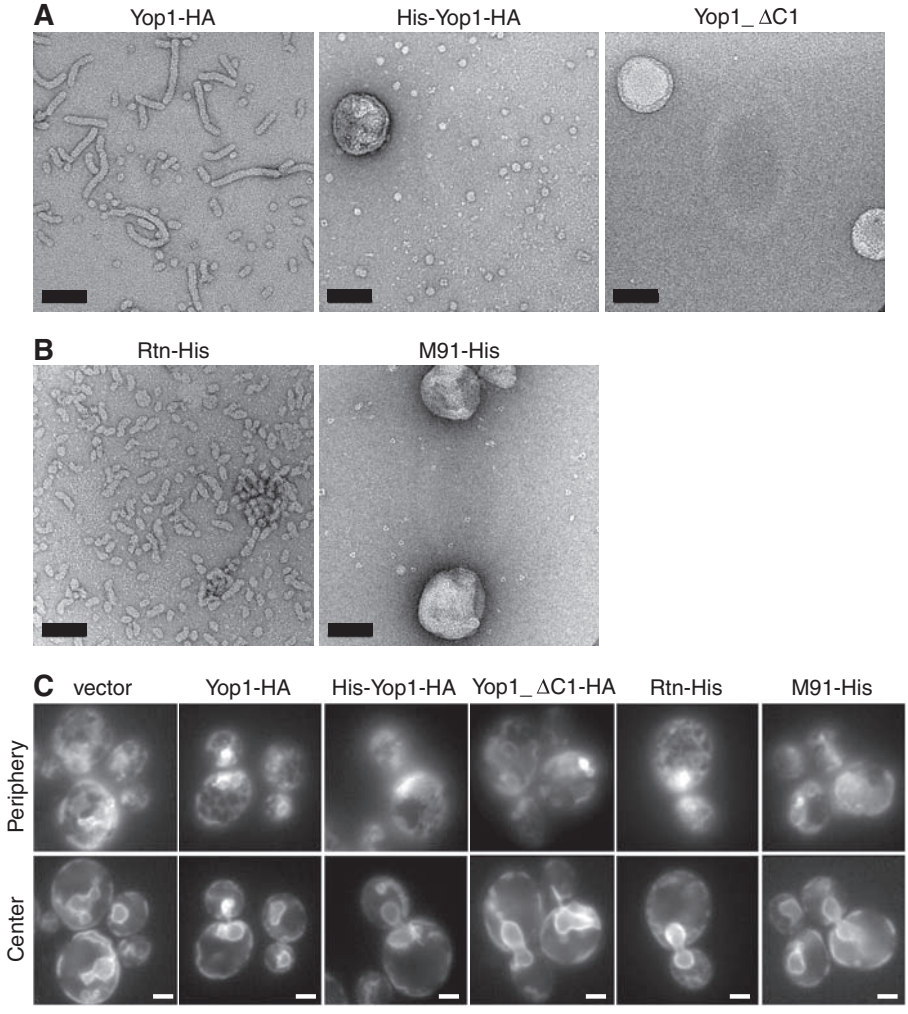

To determine the tubule-forming domain of Yop1p, the tubules were treated with increasing concentrations of trypsin. Both termini of reconstituted Yop1p were readily cleaved (fig. S4), which was consistent with their proposed localization in the cytosol. A stable fragment protected by the lipid bilayer corresponded to amino acids 24 to 165. When purified as a recombinant protein from yeast, this fragment (Yop1_ΔC2) was even more efficient in tubule formation than the full-length protein (fig. S5). However, a Yop1p fragment lacking an additional 28 residues at the C terminus (Yop1_ΔC1) was inactive (Fig. 2A). Thus, the tubule-inducing domain of Yop1p comprises the two hydrophobic segments and the intervening domain, as well as a few flanking residues.

Purified His-tagged Yop1p did not induce tubules in vitro (Fig. 2A), even though it was able to form small vesicles similar to those formed by the nontagged protein (compare Fig.1B and fig. S6C) when the detergent was diluted. We thus tested whether His-Yop1p and Yop1_ΔC1, both defective in tubule formation in vitro (Fig. 2A), were also nonfunctional in vivo. Indeed, although Yop1p without a His tag restored the tubular ER in *S. cerevisiae* cells lacking Yop1p, Rtn1p, and Rtn2p, neither His-Yop1p nor Yop1_ΔC1 was active (Fig. 2C). In addition, the His tag prevented the formation of long tubules seen with overexpression of Yop1p in wild-type cells (fig. S6A). His-Yop1p still formed ladders in cross-linking experiments and migrated at higher molecular weight in sucrose-gradient centrifugation (fig. S2C), which indicated that oligomerization alone is insufficient for tubule formation. We also identified an Rtn1p mutant (M91) that carried multiple amino acid changes and was unable to complement the triple knockout mutant in vivo (Fig. 2C); the purified His-tagged M91 protein did not form tubules in vitro, but wild-type Rtn1-His did (Fig. 2B). Thus, there is a good correlation between tubule formation in vitro and in vivo.

The narrow diameter of the tubules generated by reconstituted Yop1p was confirmed by cryo-EM analysis (Fig. 3A). The diameter was ~15 nm, somewhat smaller than the width of the flattened tubules seen by negative-stain EM (~17 nm). In vitreous ice, the outer edge of the tubules appeared much darker than their interior, verifying that the observed structures consist of a bilayer enclosing a lumen. A tubule diameter of ~15 nm was also determined in thin-section EM (Fig. 3B). Given that each lipid bilayer has a thickness of about 3 to 4 nm (*7*), the tubules have an extreme curvature, perhaps the highest achievable.

We reasoned that the in vitro tubules are narrower than those normally found in cells because they have a higher concentration of tubule-inducing protein in the lipid bilayer (by a factor of ~20). Indeed, whereas endogenous Rtn4 co-localized with the luminal protein calreticulin in mammalian cells, overexpressed Rtn4a, DP1, Rtn3c, or Yop1p squeezed calreticulin out of the tubules (Fig. 3C and fig. S7). The overexpression of reticulon in yeast or plant cells also displaced luminal proteins from the tubular ER [Fig. 3D and (*8*)]. The diameter of ER tubules in COS cells overexpressing Rtn4a was determined to be ~20 nm (Fig. 3E), significantly smaller than that of normal ER tubules (~50 nm) [(*4*) and fig. S7].

Thus, individual members of the reticulon and Yop1p (DP1) families are sufficient to induce membrane tubules. Rtn1p and Yop1p are integral membrane proteins, whereas previously identified tubule-forming proteins, such as those containing a BAR domain (*9*–*12*), are soluble. The reticulons and Yop1p (DP1) could shape the phospholipid bilayer by two mechanisms. First, the two hydrophobic hairpin segments could cause local spontaneous curvature by forming a wedge in the lipid bilayer. Second, oligomerization of these proteins could generate arcs whose shape may deform the bilayer into tubules. These mechanisms might cooperate with one another.

To illustrate the effect of arc-like protein oligomers on membrane tubule formation, we have developed a simple model. It assumes that the membrane shape is determined by the opposing effects of the protein arcs to bend the lipid bilayer and the bilayer resisting such bending (*6*). If the arcs are ordered into rings encircling a tubule, which corresponds to a maximal localization of the constraints imposed by them on the

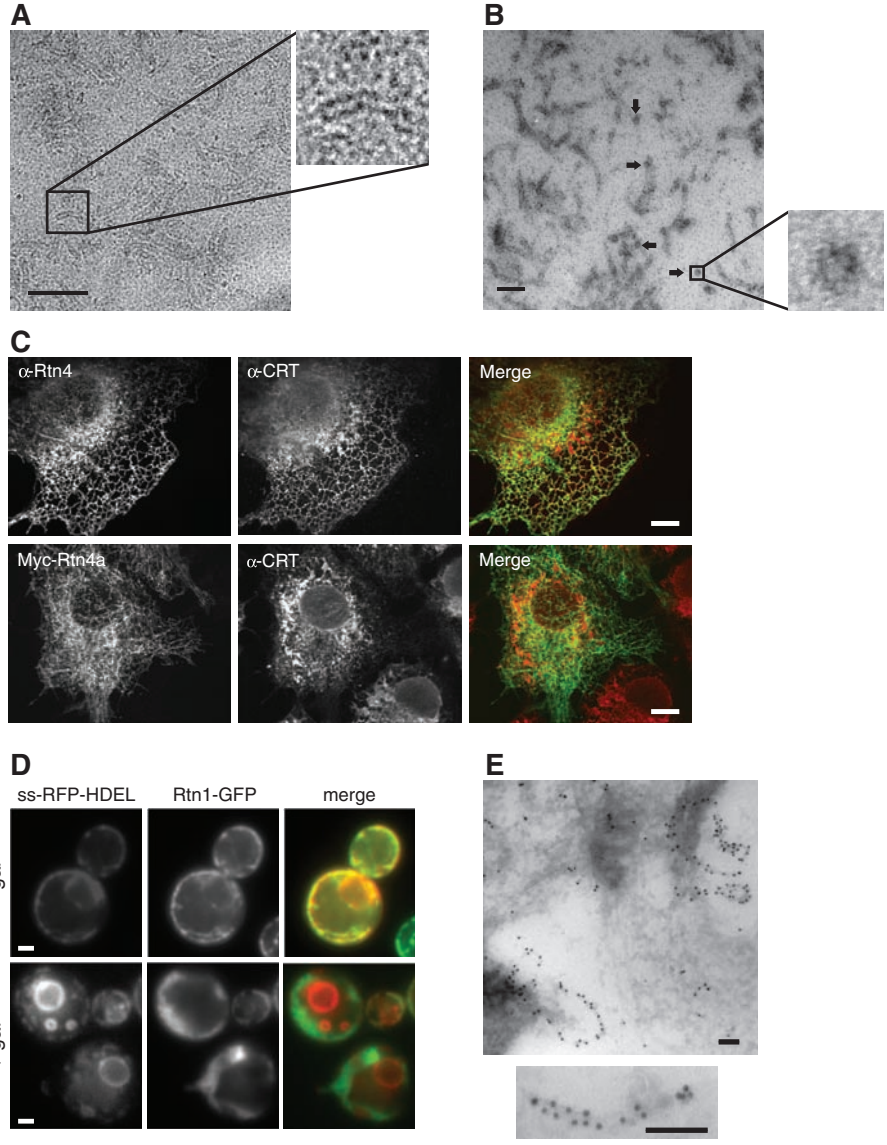

Fig. 3. Determining the diameter of tubules. (**A**) Yop1p tubules generated in vitro were analyzed by cryo-EM. Scale bar, 200 nm. (**B**) Yop1p tubules were analyzed by thin-section EM. Arrows indicate cross sections. Scale bar, 100 nm. (**C**) Nontransfected COS cells (top row) or COS cells overexpressing Myc-Rtn4a were immunostained for endogenous Rtn4 or the Myc tag (green), co-immunostained for endogenous calreticulin (red), and analyzed by confocal fluorescence microscopy. The right panels show merged images. Scale bars, 10 μm. (**D**) Yeast cells expressing a fusion of a signal sequence with the red fluorescent protein and HDEL (*26*) (ss-RFP-HDEL) and Rtn1-GFP were imaged with or without overexpression of Rtn1-HA (±gal). Scale bars, 1 μm. (**E**) Ultrathin frozen sections of COS cells expressing Rtn4a-GFP were labeled with antibodies to GFP followed by protein A–conjugated 10-nm gold. The lower panel shows a magnified image. Scale bars, 100 nm.

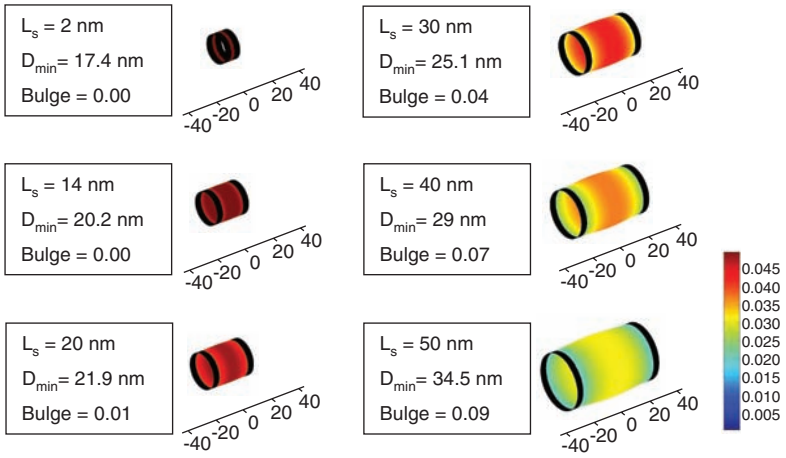

Fig. 4. Calculated shapes of membrane tubules constricted by protein rings. The barrel-shaped structures were calculated for different distances L_s between the rings. D_{min} is the minimal diameter at a ring. Bulging between rings is defined as BULGE = $(D_{max} - D_{min})/D_{min}$, with D_{max} being the maximal diameter between rings. The bending rigidity of protein and lipid were assumed to be 800 $k_BT \cdot$ nm and 20 k_BT, respectively (where k_BT = 0.6 kcal/mol is the thermal energy). The spontaneous curvature of the protein and the thickness of the protein ring were taken to be 0.13 nm^{-1} and 4 nm, respectively. The color maps represent local mean curvature of the membrane in nm^{-1}.

bilayer, a change of the distance between rings from 2 to 50 nm can explain the increase of tubule diameter from 17 nm in the in vitro experiments to ~30 nm in vivo (Fig. 4). The bulging between rings is negligible, even for relatively large distances. Almost perfect cylindrical tubules can thus be generated with the tubule-forming proteins occupying a small fraction of the total membrane surface (fig. S8). We estimate that in fact ~10% of the total tubular ER surface in *S. cerevisiae* could be occupied by the tubule-forming proteins. In reality, the arc-shaped oligomers may be distributed randomly along the tubule, and they may be disassembled actively, which would allow other ER proteins to diffuse in the plane of the membrane.

We hypothesize that the reticulons and Yop1p (DP1) use both their wedgelike shapes and their oligomerization into arcs or rings to generate the tubular ER with minimal surface coverage. Some membrane-shaping proteins, such as synaptotagmin and epsin, use only the wedging mechanism and insert hydrophobic amino acids into the outer leaflet of the bilayer (*13*, *14*), but they need to occupy a large percentage of the membrane surface to induce curvature (*13*). Other proteins, such as the F-BAR proteins and dynamins, primarily form ring- or spiral-shaped scaffolds to generate tubules (*15*–*20*). A combination of the wedging and scaffolding mechanisms, as proposed for the reticulons and Yop1p (DP1), is employed by endophilin and amphiphysin (*9*–*12*, *21*). A combination of the two mechanisms also may be used by other integral membrane proteins that shape organelles. For example, caveolin, which shapes flasklike invaginations of the plasma membrane, called caveoli, has a single hairpin membrane anchor and forms filaments or spirals on the cytoplasmic face of the organelle (*22*). The dynamin-like protein Fzo1p in yeast (Mfn in mammals) in the outer mitochondrial membrane (*23*), which is required for the maintenance of proper mitochondrial tubules, has a hairpin-shaped membrane anchor and oligomerization domains that are essential for its function (*24*, *25*). The proposed mechanisms might thus be generally used to generate organelles with high membrane curvature.

References and Notes

1. O. Baumann, B. Walz, *Int. Rev. Cytol.* **205**, 149 (2001).
2. G. K. Voeltz, W. A. Prinz, *Nat. Rev. Mol. Cell Biol.* **8**, 258 (2007).
3. S. Bernales, K. L. McDonald, P. Walter, *PLoS Biol.* **4**, e423 (2006).
4. D. W. Fawcett, *The Cell* (Saunders, Philadelphia, ed. 2, 1981).
5. G. K. Voeltz, W. A. Prinz, Y. Shibata, J. M. Rist, T. A. Rapoport, *Cell* **124**, 573 (2006).
6. Materials and methods are available as supporting material on *Science* Online.
7. K. Mitra, I. Ubarretxena-Belandia, T. Taguchi, G. Warren, D. M. Engelman, *Proc. Natl. Acad. Sci. U.S.A.* **101**, 4083 (2004).
8. N. Tolley *et al.*, *Traffic* **9**, 94 (2008).
9. K. Takei, V. I. Slepnev, V. Haucke, P. De Camilli, *Nat. Cell Biol.* **1**, 33 (1999).
10. B. J. Peter *et al.*, *Science* **303**, 495 (2004).
11. M. Masuda *et al.*, *EMBO J.* **25**, 2889 (2006).
12. J. L. Gallop *et al.*, *EMBO J.* **25**, 2898 (2006).
13. S. Martens, M. M. Kozlov, H. T. McMahon, *Science* **316**, 1205 (2007).
14. M. G. Ford *et al.*, *Nature* **419**, 361 (2002).
15. A. Frost, P. De Camilli, V. M. Unger, *Structure* **15**, 751 (2007).
16. W. M. Henne *et al.*, *Structure* **15**, 839 (2007).
17. A. Shimada *et al.*, *Cell* **129**, 761 (2007).
18. K. Takei, P. S. McPherson, S. L. Schmid, P. De Camilli, *Nature* **374**, 186 (1995).
19. J. E. Hinshaw, S. L. Schmid, *Nature* **374**, 190 (1995).
20. B. Marks *et al.*, *Nature* **410**, 231 (2001).
21. J. L. Gallop, P. J. Butler, H. T. McMahon, *Nature* **438**, 675 (2005).
22. K. G. Rothberg *et al.*, *Cell* **68**, 673 (1992).
23. G. J. Praefcke, H. T. McMahon, *Nat. Rev. Mol. Cell Biol.* **5**, 133 (2004).
24. G. J. Hermann *et al.*, *J. Cell Biol.* **143**, 359 (1998).
25. E. E. Griffin, D. C. Chan, *J. Biol. Chem.* **281**, 16599 (2006).
26. Mutations are the result of amino acid substitutions; for example, H7Y indicates that Tyr was substituted for His at position 7. Single-letter abbreviations for the amino acid residues are as follows: A, Ala; C, Cys; D, Asp; E, Glu; F, Phe; G, Gly; H, His; I, Ile; K, Lys; L, Leu; M, Met; N, Asn; P, Pro; Q, Gln; R, Arg; S, Ser; T, Thr; V, Val; W, Trp; and Y, Tyr.

27. We thank D. Moazed, B. Glick, and R. Yan for materials; T. Walz and T. Mitchison for discussions; D. Kelly and G. Skiniotis for comments; and J. F. Ménétret and M. Ericsson for help with EM experiments. C.V. and W.A.P. were supported by the NIDDK intramural program. T.A.R. is a Howard Hughes Medical Institute Investigator.

Supporting Online Material

www.sciencemag.org/cgi/content/full/319/5867/1247/DC1
Materials and Methods
Figs. S1 to S8
Table S1
References

30 November 2007; accepted 18 January 2008
10.1126/science.1153634

Leading-Edge Vortex Improves Lift in Slow-Flying Bats

F. T. Muijres,[1] L. C. Johansson,[1] R. Barfield,[1] M. Wolf,[1] G. R. Spedding,[2] A. Hedenström[1]*

Staying aloft when hovering and flying slowly is demanding. According to quasi–steady-state aerodynamic theory, slow-flying vertebrates should not be able to generate enough lift to remain aloft. Therefore, unsteady aerodynamic mechanisms to enhance lift production have been proposed. Using digital particle image velocimetry, we showed that a small nectar-feeding bat is able to increase lift by as much as 40% using attached leading-edge vortices (LEVs) during slow forward flight, resulting in a maximum lift coefficient of 4.8. The airflow passing over the LEV reattaches behind the LEV smoothly to the wing, despite the exceptionally large local angles of attack and wing camber. Our results show that the use of unsteady aerodynamic mechanisms in flapping flight is not limited to insects but is also used by larger and heavier animals.

Generating enough lift during hovering and slow forward flight is problematic according to traditional quasi–steady-state wing theory (*1*, *2*). Yet several species of small flying vertebrates are adapted to foraging using this flight mode. Insects are able to hover by using a range of possible unsteady high-lift mechanisms, including rotational circulation (*3*),